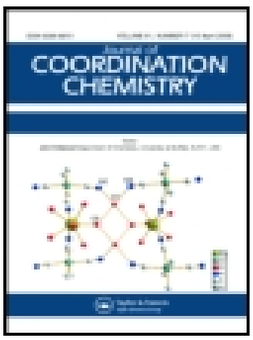

Journal of Coordination Chemistry

ISSN: 0095-8972 (Print) 1029-0389 (Online) Journal homepage: http://www.tandfonline.com/loi/gcoo20

Ternary and binary copper(II) complexes: Synthesis, characterization, ROS-inductive, proteasome inhibitory and anticancer properties

May Lee Low, Cheang Wei Chan, Pei Ying Ng, Ing Hong Ooi, Mohd Jamil Maah, Soi Moi Chye, Kong Wai Tan, Seik Weng Ng & Chew Hee Ng

To cite this article: May Lee Low, Cheang Wei Chan, Pei Ying Ng, Ing Hong Ooi, Mohd Jamil Maah, Soi Moi Chye, Kong Wai Tan, Seik Weng Ng & Chew Hee Ng (2016): Ternary and binary copper(II) complexes: Synthesis, characterization, ROS-inductive, proteasome inhibitory and anticancer properties, Journal of Coordination Chemistry, DOI: 10.1080/00958972.2016.1260711

To link to this article: http://dx.doi.org/10.1080/00958972.2016.1260711

Accepted author version posted online: 14 Nov 2016.

Publisher: Taylor & Francis
Journal: *Journal of Coordination Chemistry*
DOI: http://dx.doi.org/10.1080/00958972.2016.1260711

Ternary and binary copper(II) complexes: Synthesis, characterization, ROS-inductive, proteasome inhibitory and anticancer properties

MAY LEE LOW†, CHEANG WEI CHAN†‡, PEI YING NG†, ING HONG OOI†, MOHD JAMIL MAAH‡, SOI MOI CHYE§, KONG WAI TAN‡, SEIK WENG NG‡ and CHEW HEE NG1†

†Department of Pharmaceutical Chemistry, School of Pharmacy, International Medical University, No.126, Jalan Jalil Perkasa 19, 57000 Kuala Lumpur (Malaysia)
‡Department of Chemistry, Faculty of Science, Universiti Malaya, 50603 Kuala Lumpur (Malaysia)
§Department of Human Biology, School of Medicine, International Medical University, No.126, Jalan Jalil Perkasa 19, 57000 Kuala Lumpur (Malaysia)

Three ternary copper(II) complexes, [Cu(phen)(L-phe)Cl]·2H_2O, [Cu(phen)(L-leu)Cl]·4½H_2O, and [Cu(phen)(L-tyr)Cl]·3H_2O, and four binary copper(II) complexes, [Cu(phen)Cl_2], Cu(L-phe)$_2$·½H_2O, Cu(L-leu)$_2$·½H_2O and Cu(L-tyr)$_2$·H_2O (where phen = 1,10-phenanthroline, L-phe = L-phenylalanine, L-tyr = L-tyrosine, L-leu = L-leucine and Cl^- = chloride), were synthesized and characterized by elemental analysis, spectroscopic techniques (FTIR, UV-visible, fluorescence spectroscopy), magnetic susceptibility, molar conductivity and lipophilicity measurement. X-ray diffraction determination of a single crystal of [Cu(phen)(L-tyr)Cl] showed two independent molecules in the asymmetric unit, each with the same distorted square pyramidal geometry about copper(II). p-Nitrosodimethylaniline assay revealed that the three ternary complexes were better inducers of reactive oxygen species over time than binary complexes, $CuCl_2$ and free ligands. All the copper(II) complexes in this series inhibited the three proteolytic activities in the order Trypsin-like > Caspase-like > Chymotrypsin-like. In terms of anticancer properties, the copper(II)-phen complexes had GI50 values of less than 4 μM against MCF-7, HepG2, CNE1 and A549 cancer cell lines, more potent than cisplatin.

Keywords: Copper(II) complexes; 1,10-Phenanthroline; L-Amino acids; Reactive oxygen species; 20S Proteasome

1Corresponding author. Email: NgChewHee@imu.edu.my

1. Introduction

Cu(II) complexes have diverse biomedical applications as antimicrobial, antiviral, anti-inflammatory, enzyme inhibitors or antiprotozoal agents [1-4]. Their possible use as alternative antitumor agents is of current interest [5-7]. Uptake of copper by cancer cells has been shown to be more than that by normal cells [8]. The altered metabolism of cancer cells and the differential response between normal and cancer cells towards copper is one basis for the development of Cu(II) complexes as anticancer agents which are selective towards cancer cells [9, 10]. Another basis is that higher oxidative stress in cancer cells can allow use of compounds which can target the redox process and thereby modulate intracellular reactive oxygen species (ROS) levels [8, 11]. ROS-inducing compounds, such as β-phenylethyl isothiocyanate (PEITC) and $[Cu(phen)(c\text{-}dmg)(H_2O)]NO_3$ (c-dmg = 2,2-dimethylglycine), selectively kill the transformed cells but not normal cells, suggesting the possibility of using this strategy for improving selectivity against cancer cells [6, 12]. The selectivity was explained by reaching the "ROS threshold of initiation of apoptosis" only in cancer cells.

1,10-Phenanthroline (phen) is one of the most extensively used polypyridine ligands, and copper complexes have been found to have DNA cleaving ability [13-15]. Numerous ternary Cu(II)-phen-amino acid complexes have been synthesized and their binding to DNA studied by means of electron paramagnetic resonance [16]. The type of amino acid was found to affect the anticancer [17], antibacterial [18] and SOD-like [19] activities of the Cu(II) complexes. However, the underlying factors affecting the anticancer property of these Cu(II)-phen-amino acid complexes are seldom investigated.

It is therefore interesting to note that although the nature of ligand can have profound effect on the biological properties of metal ions, the reverse effect is also true. This "chelation effect" is a characteristic feature of metal complexes and can result in alteration of the physico-chemical and biological properties of both the ligand and metal or either one of them. The oxidation state of metal center, coordination geometry, stability, ligand lability and other characteristics will affect the chemical and biological properties of the resultant metal complexes. Our goal is to explore not only the potential use of copper compounds as anticancer agents but also the influence of various ligands on their biological activities. Thus far, Cu(II)-phen and ternary complexes focused mainly on their effects on nucleic acid activities [20-22]. We are particularly interested in the investigation of these complexes as proteasome inhibitors.

Proteasome, a multicatalytic complex involved in protein degradation, is a new validated target of anticancer and antiprotozoal compounds [23-26].

ROS-inducing property of Cu(II) salts and their complexes is of interest because of the role of ligands in modulating the ROS-inducing property of Cu(II) when bound to these ligands. Many binary and ternary Cu(II) complexes with different types of ligands can cleave DNA oxidatively in the presence of a reductant (*e.g.* ascorbic acid) or oxidant (*e.g.* hydrogen peroxide, H_2O_2) but ROS-generating ability is rarely quantitatively compared with each other and their precursor Cu(II) salts and ligands [27-29]. Therefore, to expand our work on Cu(II)-phen-aa derivatives (aa = amino acid), a series of binary and ternary copper(II) complexes with amino acids, *viz*. L-phenylalanine (L-phe), L-tyrosine (L-tyr) and L-leucine (L-leu), were synthesized and characterized to investigate the chelation effect on their reaction with H_2O_2 to yield hydroxyl radicals. These selected amino acids were chosen because they were reported to be more potent than other amino acids in their inhibition of the chymotrypsin-like activity of proteasome [30]. The anticancer properties of these complexes against breast cancer (MCF-7), liver hepatocellular (HepG2), nasopharyngeal carcinoma (CNE1) and lung tumor (A549) cell lines are compared. The correlation of their anticancer properties with their ROS generation and proteasome inhibition activities are discussed. The crystal structure of [Cu(phen)(L-tyr)Cl] is also reported herein.

2. Experimental

2.1. *Materials and instrumentation*

All chemicals and solvents were of analytical grade and used as received. The chemicals 1,10-phenanthroline and L-phenylalanine were purchased from Sigma (St Louis, US) while L-leucine and L-tyrosine were from Acros Organics. Sodium hydrogen carbonate and copper(II) chloride dihydrate were purchased from Riedal-de Haen and Friedemann Schmidt, respectively. FT-IR spectra were recorded as KBr pellets from 400-4000 cm^{-1} on a Shimadzu 8400S FT-IR spectrometer. Microanalyses were performed at the National University of Singapore. The UV-Vis spectra were recorded on a Perkin Elmer Lambda 25 (200-800 nm) spectrophotometer with a 1 cm optical path quartz cuvette. A CON 700 bench top conductivity meter (EUTECH Instruments) was used to measure the conductivity of the water-methanol (v/v 1:1) solutions of the Cu(II) compounds. The magnetic susceptibility was determined with a Sherwood Scientific

MK 1 Magnetic Susceptibility Balance at room temperature. The lipophilicity of each Cu(II) complex was determined by the shake flask method and its evaluation was based on partitioning in an octanol-water mixture. A calibration curve (using absorbance at λ_{max}) of each Cu(II) complex was used to determine the concentration of its corresponding Cu(II) complex in aqueous layer before partitioning (C_0) and in aqueous layer after partitioning (C_{aq}). Then, the log P value of each Cu(II) complex was calculated from Equation 1.

$$\text{Lipophilicity} = \log \text{P} = \log \frac{(\text{Co}-\text{Caq})}{\text{Caq}} \quad (1)$$

2.2. ***Synthesis of Cu(II) complexes***

The [Cu(phen)(aa)Cl]·xH_2O (aa: L-leu, L-phe and L-tyr) complexes were similarly prepared and the general procedure is described as follows. The $CuCl_2$·$2H_2O$ (0.17048 g, 1 mmol) was first dissolved in 20 ml of H_2O-EtOH (1:1 ratio, v/v). An equimolar amount of 1,10-phenanthroline (0.18021 g, 1 mmol) was added to the solution with continuous stirring. Then, a 20 mL solution of the L-amino acid (1 mmol) dissolved in a water-ethanol mixture was added to the solution. The pH of the resultant solution was adjusted to approximately 6.5 with $NaHCO_3$ solution. The solution was then heated and stirred for another hour and filtered while hot before further heating in a water bath (55 °C) until the volume was one-third of the original volume. The solution was allowed to evaporate at room temperature for a few hours to several days until blue crystals of the desired complexes were obtained. The products were filtered off, washed with cold ethanol and dried overnight in an oven at 60 °C. For [Cu(phen)(L-phe)Cl] synthesis, the blue precipitate that formed immediately was not the desired product. Blue crystals, which crystallized from the filtrate, were established to be the desired [Cu(phen)(L-phe)Cl] complex.

[Cu(phen)Cl_2] was previously synthesized by Detoni *et al*. [31], but the current synthesis of this complex involved a slightly modified procedure of heating for 30 min an ethanolic solution containing $CuCl_2$·$2H_2O$ and 1,10-phenanthroline at metal-ligand ratio of 1:1. The $Cu(aa)_2$ (aa: L-leu, L-phe and L-tyr) complexes were prepared by reacting freshly prepared copper(II) hydroxide with the respective amino acid, in the same way as synthesizing similar $Cu(aa)_2$ complexes [32, 33].

[*Cu(phen)(L-phe)Cl*]·3H_2O (Yield = 53%) Elemental analysis for $C_{21}H_{24}ClCuN_3O_5$: Calcd. C 50.70, H 4.86, N 8.45; Found C 50.24, H 4.41, N 8.43. IR: ν (cm^{-1}) = 3462 (b) 3215 (m) 3118 (m) 1614 (s) 1405 (m) 853 (m) 721 (m). UV-Vis in water-ethanol (1:1): λ_{max} in nm (ε in mol^{-1}·dm^3 cm^{-1}) = 224 (29081), 273 (28981), 294 (9046), 620 (61). Magnetic moment: μ_{eff} (B.M.) = 1.80. Lipophilicity (log $P_{oct/water}$) = -1.37.

[*Cu(phen)(L-leu)Cl*]·4½H_2O (Yield = 22%) Elemental analysis for $C_{18}H_{29}ClCuN_3O_{6.5}$: Calcd. C 44.08, H 5.96, N 8.57; Found C 43.95, H 5.51, N 8.56. IR: ν (cm^{-1}) = 3405 (b) 3245 (m) 2960 (m) 1620 (s) 1397 (m) 852 (m) 721 (m). UV-Vis in water-ethanol (1:1): λ_{max} in nm (ε in mol^{-1}·dm^3 cm^{-1}) = 223 (19625), 272 (19271), 294 (5027), 620 (52). Magnetic moment: μ_{eff} (B.M.) = 1.93. Lipophilicity (log $P_{oct/water}$) = -1.90.

[*Cu(phen)(L-tyr)Cl*]·3H_2O (Yield = 74%) Elemental analysis for $C_{21}H_{24}ClCuN_3O_6$: Calcd. C 49.13, H 4.71, N 8.18; Found C 48.96, H 4.12, N 8.22. IR: ν (cm^{-1}) = 3433 (b) 3210 (m) 3118 (m) 1612 (s) 1409 (m) 849 (m) 723 (m). UV-Vis in water-ethanol (1:1): λ_{max} in nm (ε in mol^{-1}·dm^3 cm^{-1}) = 224 (31982), 273 (26659), 294 (7933), 620 (62). Magnetic moment: μ_{eff} (B.M.) = 1.66. Molar conductivity: Λ ($ohm^{-1}cm^2mol^{-1}$) = 12.80. Lipophilicity (log $P_{oct/water}$) = -1.69.

[*Cu(phen)*Cl_2] (Yield = 37%) Elemental analysis for $C_{12}H_8Cl_2CuN_2$: Calcd. C 45.80, H 2.56, N 8.90; Found C 45.29, H 2.47, N 8.83. IR: ν (cm^{-1}) = 3055 (m) 1624 (m) 855 (s) 721 (s). UV-Vis in water-ethanol (1:1): λ_{max} in nm (ε in mol^{-1}·dm^3 cm^{-1}) = ~221 (27566, sh), 272 (28745), 294 (8228), 715 (30). Magnetic moment: μ_{eff} (B.M.) = 1.73. Lipophilicity (log $P_{oct/water}$) = -1.44.

Cu(L-phe)$_2$·2H_2O (Yield = 80%) Elemental analysis for $C_{18}H_{21}CuN_2O_{4.5}$: Calcd. C 53.92, H 5.28, N 6.99; Found C 53.82, H 4.91, N 7.00. IR: ν (cm^{-1}) = 3452 (b) 3250 (m) 1620 (s) 1393 (m). UV in water-ethanol (1:1): λ_{max} in nm (ε in mol^{-1}·dm^3 cm^{-1}) = 234 (2485). Magnetic moment: μ_{eff} (B.M.) = 1.87. Lipophilicity (log $P_{oct/water}$) = -0.47.

Cu(L-leu)$_2$·2H_2O (Yield = 84%) Elemental analysis for $C_{12}H_{25}CuN_2O_{4.5}$: Calcd. C 43.30, H 7.57, N 8.42; Found C 43.58, H 7.09, N 8.51. IR: ν (cm^{-1}) = 3459 (b) 3244 (m) 1619 (s)

1397 (m). UV-Vis in water-ethanol (1:1): λ_{max} in nm (ε in mol^{-1} dm^3 cm^{-1}) = 232 (2284). Magnetic moment: μ_{eff} (B.M.) = 1.79. Lipophilicity (log $P_{oct/water}$) = -0.42.

Cu(L-tyr)$_2$·H$_2$O (Yield = 75%) Elemental analysis for $C_{18}H_{22}CuN_2O_7$: Calcd. C 48.92, H 5.02, N 6.34; Found C 48.68, H 4.71, N 6.41. IR: *ν* (cm^{-1}) = 3485 (b) 3284 (m) 1603 (s) 1383 (m). UV-Vis in water-ethanol (1:1): λ_{max} in nm (ε in mol^{-1} dm^3 cm^{-1}) = 224 (17077), 275 (1794). Magnetic moment: μ_{eff} (B.M.) = 1.94. Lipophilicity (log $P_{oct/water}$) = -1.34.

2.3. *X-ray crystallography*

Dark blue crystals of [Cu(phen)(L-tyr)Cl]·2H$_2$O formed after the reaction mixture was allowed to evaporate slowly at room temperature for one week. X-ray diffraction data for a blue prismatic crystal, of size 0.40 × 0.40 × 0.10 mm, were collected at -173 °C on a SuperNova Dual diffractometer (Agilent Technologies) equipped with an Atlas detector using MoK_α radiation (λ = 0.71073 Å). CrysAlis PRO [34] software was used for data collection, cell refinement and data reduction. The structure was solved by direct-methods using SHELXS97 [35] and refined by a full-matrix least-squares procedure SHELXL2014/7 [36].

2.4. *PNDA assay*

To quantify the amount of ·OH radicals produced by reaction of the Cu(II) complexes with hydrogen peroxide in borate buffer at pH 7.5, a previously reported spectrometric assay using p-nitrosodimethylaniline (PNDA) was used [37, 38]. The percentage bleaching of the PNDA was calculated using the formula:

$$\% \text{ Bleaching of PNDA} = 100 \times (A_o - A_t)/A_o$$

A_o = absorbance of sample with PNDA at 440 nm at t = 0

A_t = absorbance of sample with PNDA at 440 nm at any time, t

A total volume of 300 µL of each assay mixture was obtained by adding sequentially 90 µL of test compound (30 µM), 141.6 µL of borate buffer (33 mM, pH7.5), 50.4 µL of PNDA (42 µM) and 18 µL of H_2O_2 (60 mM) in a 96-well transparent plate. The absorbance reading at 440 nm

was taken immediately after the addition of hydrogen peroxide by using SpectraMax M5 multi-mode microplate reader, and these readings were read at intervals of 5 minutes for 4 h.

2.5. *Proteasome inhibition*

Fluorogenic substrates Suc-Leu-Leu-Val-Tyr-AMC, Boc-Leu-Arg-Arg-AMC and Z-Leu-Leu-Glu-AMC (UBPBio USA) were used to measure chymotrypsin-like (CT-L), trypsin-like (T-L) and caspase-like (C-L) activities of the 20S proteasome, respectively. A total volume of 100 μL of each assay mixture, consisting of 14 μL of activated purified 20S mouse proteasome (2 nM/well; R&D Systems USA), with 20 μL of 20 μM fluorogenic peptide substrate (at 4 μM/well), an appropriate volume of buffer (50 mM Tris-HCl, pH 7.5) and appropriate volume of test compound at indicated concentration (2.5, 5, 10, 20, 30 and 40 μM) in a 96-well fluorometer plate, was incubated for 24 h at 37 °C. After incubation, fluorescence of the cleaved fluorogenic groups was measured by using a SpectraMax M5 multimode microplate reader with an excitation filter of 380 nm and an emission filter of 460 nm. Activity (%) of each site was calculated using the equation below.

Activity (%) = (optical density of sample)/(optical density of control) × 100%

Changes in fluorescence were calculated against non-treated controls and plotted with statistical analysis using Microsoft Excel. The concentration (μM) of samples that induced 50% inhibition of the 20S's three proteolytic sites were determined using the plot of activity (%) of each site against concentration of test sample.

2.6. *In vitro cytotoxicity assay*

MCF-7 (human breast cancer cells possessing nuclear estrogen receptor), HepG2 (human hepatocellular liver carcinoma cell line), CNE1 (a highly differentiated nasopharyngeal carcinoma cell line) and A549 (human lung adenocarcinoma epithelial cell line) were obtained from the International Medical University cell bank. The cell lines were cultured in DMEM (high glucose; Gibco/Life Technologies) medium supplemented with 10% fetal calf serum. Different series of wells in 96-well flat bottom tissue culture plates were pipetted with 100 μL of cells of their respective cell lines. The seeding densities of the wells in each series were the same but they varied with the cell line. The seeding densities were approximately 15,000 cells for

MCF-7, 6,000 cells for HepG2, 3,000 cells for CNE1 and 6,000 cells for A549 per. After seeding, the cells in the plates were allowed to adhere and incubate at 37 °C (5% CO_2 and 95% air) overnight. Then, the culture media of these wells were discarded. Each series of wells were added with test compound and the wells were diluted with culture medium to give 0, 0.1, 2.5, 5 and 10 μM of test compound. The total volume of each mixture in each well was 100 μL. The series of tested compound mixtures were done in four replicates. The negative control wells had only 100 μL of 10% FBS-DMEM media. After incubating the 96-well plates for another 48 h, the culture media of the wells in the plates were discarded. These wells were then titrated with 3-(4,5-dimethylthiazol-2-yl)-2,5-diphenyltetrazolium bromide (MTT) to determine the viability of the cells [39]. Briefly, 20 μL of MTT solution (5 mg/mL in PBS) was added to each well and the 96-well plates were incubated for an additional 4 h to allow metabolism of MTT by cellular mitochondrial dehydrogenases of live cells. The medium and excess MTT in each well were aspirated and the formazan crystals formed were solubilized by adding 80 μL of DMSO. The absorbance of purple formazan, corresponding to the number of viable cells, was measured at 570 nm using the Versamax microplate reader with background subtraction at 630 nm. The results were analyzed using SOFTmax® Pro software. Using the absorbance value at 0-day as the initial optical density, the percentage growth curves were constructed and the GI50 (concentration that produces 50% growth inhibition), TGI (concentration that produces total growth inhibition of cytostatic effect) and LC50 (-50% growth: lethal concentration or 'net cell killing' or cytotoxicity parameter) values were interpolated from the curves. The growth percentages were determined using the formulas listed below.

$$\% \text{ of cell growth} = [(A_T - A_0) / (A_C - A_0)] \times 100 \qquad \text{if, } A_T \geq A_0$$

or

$$\% \text{ of cell growth} = [(A_T - A_0) / (A_0)] \times 100 \qquad \text{if, } A_T < A_0$$

A_T = Absorbance of treated cells

A_C = Absorbance of control cells

A_0 = Absorbance on 0 day

3. Results and discussion

3.1. *Crystal structure of [Cu(phen)(L-tyr)Cl]·2H$_2$O*

Crystal data and refinement parameters of [Cu(phen)(L-tyr)Cl]·2H_2O are given in table 1. The complex crystallized in the monoclinic, non-centrosymmetric space group of $P2_1/c$ with the unit cell parameters a = 11.6174(8) Å, b = 16.2035(12) Å, c = 11.7564(9) Å with β = 102.0610(7)°. The crystal contains two independent [Cu(phen)(L-tyr)Cl] complex molecules (figure 1a and 1b) with different bonds and bond angles, similar to the crystal of [Cu(phen)(L-tyr)(H_2O)]ClO_4·2½H_2O which has two independent [Cu(phen)(L-tyr)(H_2O)]$^+$ cations [40]. In both crystals, the two independent units (molecules or cations) have the same distorted square pyramidal structure about Cu(II). However, they differ in having different apical ligands, which is chloride in the former and aqua in the latter. Such distorted square pyramidal structures are typical of many ternary Cu(II)-phen-amino acid complexes [17, 41, 42].

ORTEP plots of the two independent molecules of [Cu(phen)(L-tyr)Cl] with atomic numbering scheme are shown in figures 1a and 1b. In comparison to the apical bonds of the two independent [Cu(phen)(L-tyr)(H_2O)]$^+$ ions (Cu(A)-O(1W) lengths: 2.24(2) Å and 2.25(2) Å, respectively) [40], those of [Cu(phen)(L-tyr)Cl] are significantly longer (Cu-Cl bond lengths: 2.5146(18) and 2.543(4) Å, respectively). The molecule 1(a) (figure 1a) shows intramolecular aromatic ring stacking interactions between the side chain aromatic ring of the coordinated L-tyr and Cu(II)-coordinated aromatic moiety [N3-C21-C10-N2-Cu(1)] of the phen ligand. The aromatic ring of the L-tyr is located approximately parallel to the coordination plane with the intramolecular stacking having an average spacing of 3.3736 Å. This stacking distance in [Cu(phen)(L-tyr)Cl] is comparable with those for Cu(phen)(L-tyr), Cu(bpy)(L-trp) (bpy = bipyridine; trp = tryptophanate), Cu(phen)(L-trp) and Cu(bpy)(L-tyr) complexes with distances of 3.38, 3.67, 3.51 and 3.35 Å, respectively [40]. Again, a close contact between Cu(II) and the carbon of the side chain aromatic ring of the L-tyr [Cu(1)….C(4) 3.286 Å] is observed; the other molecule 1(b) (figure 1b) does not exhibit such intramolecular aromatic ring stacking interaction. The plane of the aromatic ring of L-tyr is approximately perpendicular to the coordination plane formed by CuN_3O atoms with an angle of 80.40°. Selected bond lengths and angles are depicted in table 2.

3.2. *Characterization of Cu(II) complexes*

The ternary Cu(II) complexes showed two characteristic FT-IR bands (856-868 and 720-725 cm^{-1}) of coordinated phen ligand [43]. The presence of two bands at 1636-1626 and 1394-1382 cm^{-1}, attributed to the carboxylate ν_{COO-} asymmetric and symmetric stretching frequencies, respectively, are consistent with monodentate coordination of the amino acids to Cu(II) [19]. The bands at 3264-3239 and 3125-3116 cm^{-1} are due to N-H vibration of the coordinated amino group. Taken together, the ternary Cu(II) complexes can be formulated as $[Cu(phen)(aa)Cl]\cdot xH_2O$ (aa = L-phe, L-tyr, L-leu, x = number of water molecules). The binary $Cu(aa)_2\cdot xH_2O$ complexes and $Cu(phen)Cl_2$ also show similar distinctive bands corresponding to coordination of only the amino acids or the phen ligand. A broad peak at ~3455 cm^{-1} ascribed to ν_{OH}, indicating presence of coordinated or lattice water, is also observed in spectra of all complexes except for $[Cu(phen)Cl_2]$. The elemental analytical data agree well with the proposed formulas of the Cu(II) complexes.

The room temperature magnetic moment values (1.66-1.92 B.M.) of the ternary and binary complexes ($[Cu(phen)(L\text{-}phe)Cl]\cdot 3H_2O$, 1.80 B.M.; $[Cu(phen)(L\text{-}leu)Cl]\cdot 4½H_2O$, 1.93 B.M.; $[Cu(phen)(L\text{-}tyr)Cl]\cdot 3H_2O$, 1.66 B.M.; ($[Cu(phen)Cl_2]$, 1.73 B.M.; $Cu(L\text{-}phe)_2\cdot ½H_2O$, 1.87 B.M.; $Cu(L\text{-}leu)_2\cdot ½H_2O$, 1.79 B.M.; $Cu(L\text{-}tyr)_2.H_2O$, 1.94 B.M.) are similar to those of other Cu(II) complexes with d^9 electron configuration [44]. Except $[Cu(phen)(L\text{-}tyr)Cl]\cdot 3H_2O$, all the other Cu(II) complexes have magnetic moments greater than the spin-only value of 1.73 B.M. which is typical of Cu(II) (d^9) with one unpaired electron. These Cu(II) complexes have magnetic moments greater than 1.73 B.M. because of significant contribution of angular momentum to their respective magnetic moments. However, the significantly lower value of the magnetic moment (1.66 B.M.) of $[Cu(phen)(L\text{-}tyr)Cl]\cdot 3H_2O$, compared to the spin-only value of 1.73 B.M., suggests weak antiferromagnetic spin-spin coupling interaction between copper(II) ions [45, 46]. The Cu(II)-Cu(II) interaction could be facilitated by the existence of hydrogen bonding network linking the chlorido ligand of a [Cu(phen)(L-tyr)Cl] molecule, the lattice water molecules and chlorido ligand of an adjacent [Cu(phen)(L-tyr)Cl] molecule, *i.e.* magnetic interaction *via* a Cu-Cl….(H_2O)….(H_2O)…Cl-Cu pathway (figure 2). Mechanism involving such intermolecular hydrogen bonding in the magnetic exchange interactions of metal centers has only recently been discovered and established [45, 47-50]. Hitherto, magnetic exchange interactions

have acted *via* direct and superexchange mechanisms between metal centers or metal centers and various ligands [51].

3.3. *Aqueous solution of Cu(II) complexes*

The nature and stability of the Cu(II) complexes in aqueous solution is an important prerequisite for evaluation of their biological activity. UV and molar conductivity measurements were carried out at 0, 24 and 48 h. Electronic spectra of the Cu(II) complexes in water-ethanol (1:1 ratio, 30 μM) were recorded from 200-800 nm. For [Cu(phen)(aa)Cl] complexes and [Cu(phen)Cl_2], the spectra showed strong bands at *ca*. 224 nm and 272 nm which are characteristic of coordinated phen [41, 43]. The intensity and wavelength of these bands in the UV region did not change over 48 h, suggesting no dissociation of phen in the Cu(II)-phen complexes.

The visible spectral λ_{max} (nm) of the aqueous solutions of the Cu(II)-phen complexes (molar extinction coefficient, ε in $mol^{-1}\,dm^3\,cm^{-1}$)] are 715 (30) for [Cu(phen)Cl_2], 620 (61) for [Cu(phen)(L-phe)Cl], 620 (52) for [Cu(phen)(L-leu)Cl] and 620 (62) for [Cu(phen)(L-tyr)Cl]. Except for [Co(phen)Cl_2], the visible bands of the Cu(II)-phen complexes are due to d–d transitionS, which are similar to those (λ_{max} in the range 610–623 nm) determined for aqueous solutions of other [Cu(phen)(aa)(H_2O)]NO_3 (aa = amino acid) and *bis*(aminoacidato)copper(II) complexes, Cu(aa)$_2$ [32, 41, 43]. The molar extinction coefficients (ε values) are (20 – 60 $mol^{-1}\,dm^3\,cm^{-1}$) suggestive of distorted octahedral geometry about Cu(II) [52]. Again, the intensity and wavelength of these d-d bands remained practically unchanged over 48 h, suggesting no change in coordination sphere and no aquation. In contrast, aqueous solution of $CuCl_2$ has the same d-d transition band at 813 nm, typical of hydrated copper(II) ions. As expected, substitution of the coordinated water in $[Cu(OH_2)_6]^{2+}$ by stronger field ligands, phen and amino acid to form the corresponding $[Cu(phen)(ala)(H_2O)]^{2+}$ shifted the d-d transition to shorter wavelength [41, 43]. [Cu(phen)Cl_2] has longer λ_{max} than [Cu(phen)(aa)Cl] complexes as it has only two coordinated nitrogens compared to three in the latter.

The molar conductivities of 1 mM aqueous solutions of the three [Cu(phen)(aa)Cl]·xH_2O complexes in water-ethanol (table 3) are very similar (39-47 S cm^2 mol^{-1}), and they are typical of 1:1 electrolytes [41, 43]. This suggests that each of these complexes dissociated to yield the same copper(II) complex cation, $[Cu(phen)(aa)]^+$ or $[Cu(phen)(aa)(H_2O)]^+$, and the chlorides upon dissolution in aqueous solution. Within 48 h, their molar conductivities remained practically

unchanged, suggesting no dissociation of aa^- ligand. The 1 mM [Cu(phen)Cl_2] aqueous solution has a molar conductivity of 123 S cm^2 mol^{-1} which is similar to that of $Cu(NO_3)_2$ (a 2:1 electrolyte) with a molar conductivity of about 140 S cm^2 mol^{-1}, suggesting dissociation of each complex molecule into hydrated $[Cu(phen)]^{2+}$ and $2Cl^-$ ions [41]. Its molar conductivity values remained the same for 48 h, and this suggests no dissociation of the cation. Molar conductivities of the $Cu(aa)_2$ complexes could not be determined and compared because of poor solubility.

The more dilute aqueous solutions of $Cu(aa)_2 \cdot xH_2O$ complexes (100 μM) have molar conductivities of 25-30 S cm^2 mol^{-1}, indicating their non-electrolyte nature [53, 54]. Similarly, these values did not change appreciably over 48 h, suggesting no or very little dissociation of the coordinated anionic amino acid.

3.4. *Hydroxyl radical production*

For living organisms, copper is an important micronutrient [55, 56] while H_2O_2, a potentially harmful by-product of metabolism, is now known to be a second messenger in cellular signal transduction [57]. Both are tightly regulated, as accumulation gives rise to pathogenesis of various diseases. However, copper and Cu(II) compounds can catalyze the conversion of H_2O_2 to more harmful hydroxyl radicals, •OH.

The reaction of H_2O_2 with equimolar concentration of the Cu(II) complexes to yield •OH radicals was monitored by measuring the absorbance of PNDA which reacted quantitatively (1:1 mol ratio) with the •OH radicals produced. To compare production of •OH radicals by the compounds, the absorbance of PNDA (at 440 nm) was measured at 20 minute intervals over a period of 4 h. The PNDA absorbance of each reaction mixture decreased with time (figures 3a and 3b) and the slope of the curve is a measure of the rate of production of •OH radicals. The percentage bleaching of the PNDA can also be used to compare the production of •OH radicals of the Cu(II) complexes (table 4). $CuCl_2$ and the ligands are also tested under the same conditions for comparison.

The absorbance of PNDA remained almost the same for the free ligands throughout the 4 h duration (data not shown). Those for $CuCl_2$ and binary Cu(II) complexes decreased slowly with time, in contrast with those of ternary Cu(II) complexes, indicating slow production of hydroxyl radicals. This suggested that chelation of both the amino acid and the phen to Cu(II) in each of the ternary Cu(II) complexes significantly enhanced the rate of production of •OH.

Within the first 120 minutes, the rates of decrease of PNDA absorbance are about the same for both [Cu(phen)(L-leu)Cl] and [Cu(phen)Cl_2] but they are significantly faster than those of [Cu(phen)(L-phe)Cl] and [Cu(phen)(L-tyr)Cl] (figure 3b). Translating these into rate of production of •OH, the Cu(II) complexes can be arranged in order of decreasing rate of production of •OH as [Cu(phen)(L-leu)Cl] $\underline{\sim}$ [Cu(phen)Cl_2] > [Cu(phen)(L-phe)Cl] > [Cu(phen)(L-tyr)Cl]. Obviously, the type of amino acid affects the ability of the Cu(II)-phen complexes in generating •OH. However, after 120 min until 240 min, total bleaching of PNDA is the highest for Cu(phen)(L-phe)Cl and subsequently Cu(phen)(L-tyr)Cl (figure 3b; table 4). Chelation of these ligands in these Cu(II) complexes have obviously resulted in the lowering of the redox potential of the Cu(II), indicating that reduction of Cu(II) to Cu(I) is easier, and consequently Cu(I) is generated faster. Oxidation of Cu(I) to Cu(II) by H_2O_2 then yields •OH radicals. Such Cu(II)/Cu(I) redox cycling [37] produces •OH and other reactive oxygen species (ROS), which can damage biomolecules within cells [9, 58]. However, this can be attenuated, to some extent, by the antioxidant system of the organism.

3.5. *20S Proteasome inhibition*

Proteasome is responsible for degradation of most cellular proteins and its dysregulation is responsible for pathogenesis of many diseases in humans. Therefore, proteasome inhibitors can be used to treat a wide range of diseases such as cancer, bacterial and protozoan infections [25, 59-63]. The 20S proteasome which is the cylindrical core of the multicatalytic 26S proteasome complex has three proteolytic sites, *viz*. Chymotrypsin-like (CT-L), Trypsin-like (T-L) and Caspase-like (C-L) sites. Although different Cu(II) complexes are known to inhibit proteasome, their "proteasome inhibition profile" in terms of these three proteolytic sites has not been investigated [24, 64]. The present study is part of our continuous effort to characterize the proteasome inhibition profile of Cu(II)-phen-aa and other metal complexes by monitoring the degradation of fluorogenic (FL) substrates by purified 20S mouse proteasome treated with test compounds. Different series of proteasome mixtures containing respective substrates were incubated with increasing concentration of Cu(II) salt, ligands or Cu(II) complexes up to 40 µM. The IC_{50} value, *i.e*. the concentration that inhibits 50% of the proteasome activity, of each test compound for each proteolytic site was determined, and the results are tabulated in table 5.

The three amino acids (leu, phe and tyr), among the twenty amino acids, were reported to be capable of strongly inhibiting CT-L activity at normal serum concentrations, and the inhibition was concentration dependent [30]. However, our evaluation found these three ligands to be poor inhibitors of the three proteolytic sites of 20S proteasome as their IC_{50} values were higher than 40 μM. No comparison could be made as the concentrations of the amino acids in the former case were not stated, although it was mentioned that the concentration of the amino acids used were five times those in normal plasma. A normal plasma has 103, 38 and 35 μM of leu, phe and tyr, respectively [65]. All the Cu(II) compounds inhibited the three proteolytic sites differently in the order of Trypsin-like > Caspase-like > Chymotrypsin-like. $CuCl_2$ is a potent inhibitor of 20S proteasome compared to the Cu(II) complexes, suggesting that the proteasome inhibitory property of Cu(II) complexes can be attributed to Cu(II). However, the biological application of the free Cu(II) salt is limited as it has been reported to have poor cellular uptake [24, 66]. The significant role played by complexation in enhancing the lipophilicity and subsequently increased cell-penetration and bioactivity of compounds has been previously highlighted [67-69]. Considering that the IC_{50} values of [Cu(phen)(L-leu)]Cl, the binary Cu(II) complexes with amino acids and $CuCl_2$ towards the T-L site are similar, this implies that the Cu(II) complexes will be better T-L inhibitors than $CuCl_2$ for whole cells. There is also potential application for a selective T-L inhibitor as such compounds have been found to be useful in sensitizing cancer cells towards inhibitors (*e.g*. bortezomib and carfilzomib) of the CT-L sites [70]. Therefore, while the chymotrypsin-like sites are the major drug targets in cancer, co-targeting trypsin-like site increases cytotoxicity of proteasome inhibitors [71]. In fact, it is now realized that co-inhibition of caspase-like or trypsin-like sites is needed. Although chymotrypsin-like site had been considered rate limiting in protein breakdown, trypsin-like and caspase-like sites were not considered drug targets until the surprising observation was made that inhibition of chymotrypsin-like site alone is not sufficient to block protein degradation in HeLa cells [72]. Another interesting result from this study is that the ability of the Cu(II) complexes to inhibit the CT-L activity is much reduced (by about 2.5 – 6, or more) compared with that of Cu(II) salt. Generally, the Cu(II) compounds can be arranged in order of decreasing CT-L inhibitory property as $CuCl_2$ > $Cu(aa)_2$ (except $Cu(L\text{-}phe)_2$) > Cu(II)-phen complexes (except [Cu(phen)(L-tyr)Cl]). Further analysis of the data in table 4 indicated that both phen and the amino acid significantly affect the CT-L and C-L inhibitory properties of the Cu(II) complexes. However,

these two ligands have little influence on the ability of these complexes in inhibiting T-L activity.

3.6. *MTT assay results*

The concern over acquired drug resistance and serious side-effects of current anticancer drugs, in the midst of the rise of cancer and its economic cost, drives the effort to develop better alternatives [73, 74]. A slightly modified method of the National Cancer Institute was used to study the anticancer property of the copper(II) complexes (incubated with cancer cells for 48 h) which involves replacing the sulforhodamine B with MTT [75]. This allows determination of the concentration of test compound for 50% growth inhibition (GI_{50}), total growth inhibition (TGI) and 50% lethal dose (LD_{50}) (table 6). Cu(II) complexes with phen ligand (low GI_{50} and LD_{50} values; < 10 μM) showed better anticancer properties than the binary Cu(II) complexes with amino acids against the four different cancer cell lines tested (MCF-7, HepG2, CNE1 and A549). The four complexes have similar GI50 values (< 4 μM). Comparing GI50 values with the published IC_{50} values (48 h incubation) of cisplatin on MCF-7 (12-25 μM) [76,77], HepG2 (16 μM), CNE1 (15 μM) and A549 (16 μM) [78], we conclude that our Cu(II)-phen complexes (GI50 < 4 μM) are more potent. The four Cu(II)-phen complexes are both cytostatic (inhibit growth; GI50) and cytotoxic (induce cell death; LD50) towards these cell lines. One possible cause of higher potency of this set of Cu(II)-phen complexes is the higher rate or amount of ·OH production (figure 2). Their GI50 values are similar and this may be due to the fact that their productions of ·OH radicals are very similar. This is consistent with what is known about the mode of action of anticancer copper(II) complexes, which can induce apoptosis through ROS-mediated mitochondrial pathway [6, 54, 79]. Nonetheless, we could not correlate between the differential proteasome inhibition by the Cu(II) complexes and their anticancer properties.

4. Conclusion

The potential of copper(II) complexes replacing cisplatin as clinical anticancer drugs, with higher potency, less toxic side-effects and ability to overcome drug resistance, seems feasible. Numerous copper complexes, including those reported herein, are reported to have GI50 values which are comparable or better than cisplatin [80-83]. The four Cu(II)-phen complexes in this study have GI50 values of less than 4 μM against MCF-7, HepG2, CNE1 and A549 cancer cell

lines, and are more potent than cisplatin (with GI50 values in the range 12 – 25 μM). Although the potency of metal complexes does vary with the type of cancer cells, some copper(II)-phen complexes ([Cu(o-phthalate)(phenanthroline) and [Cu(phen)(aa)(H_2O)]NO_3 where aa = methylated gly] have recently been reported to have broad spectrum activity, effective against a wide range of cancer cell lines in the NCI60 panel [84, 85]. Their different modes of action include ROS-induced apoptosis, cell cycle arrest, proteasome inhibition, lowering of mitochondrial membrane potential, DNA damage, covalent binding with DNA and topoisomerase inhibition [41, 54, 80-86]. PNDA assay, as used in the current study, is an easy way of comparing ROS-inducing property of anticancer copper(II) complexes. Furthermore, comparing the extent of inhibition of the three proteolytic sites of the proteasome of such copper(II) complexes is crucial as it was only mentioned that apoptosis-induction is triggered solely by inhibition of the chymotrypsin-like site of the proteasome by copper(II) complexes [87-89]. It is now realized that co-inhibition of one or all of the other two proteolytic sites could increase the cytotoxicity of proteasome inhibitors or completely block protein degradation [70-72].

Supplementary material

The crystallographic data, CCDC 1431746, can be obtained free of charge from the Cambridge Crystallographic Data Centre via http://www.ccdc.cam.ac.uk/conts/retrieving.html, or from the Cambridge Crystallographic Data Center, 12 Union Road, Cambridge CB2 1EZ, UK; Fax: (+44) 1223–336-033; or E-mail at deposit@ccdc.cam.ac.uk.

Acknowledgements

The authors would like to thank MOSTI (eSc grant No. 02-02-09-SF0036) and S.W. Ng wishes to acknowledge the use of grant No. UM.C/HIR-MOHE/SC/03) for supporting this study.

References

[1] R. Kumar, S. Obrai, A.K. Jassal, M.S. Hundal, J. Mitra, S. Sharma. *J. Coord. Chem.*, **68**, 2130 (2015).

[2] C. Duncan, A.R. White. *Metallomics*, **4**, 127 (2012).

[3] P. Szymański, T. Frączek, M. Markowicz, E. Mikiciuk-Olasik. *Biometals*, **25**, 1089 (2012).

[4] A. Juneja, T.S. Macedo, D.R. Magalhaes Moreira, M.B. Pereira Soares, A.C. Lima Leite, J.K.A. Lemoine Neves, V.R. Alves Pereira, F. Avecilla, A. Azam. *Eur. J. Med. Chem.*, **75**, 203 (2014).

[5] S. Banerjee, A.R. Chakravarty. *Acc. Chem. Res.*, **48**, 2075 (2015).

[6] C.H. Ng, S.M. Kong, Y.L. Tiong, M.J. Maah, N. Sukram, M. Ahmad, A.S.B. Khoo. *Metallomics*, **6**, 892 (2014).

[7] M.L. Low, G. Paulus, P. Dorlet, R. Guillot, R. Rosli, N. Delsuc, K.A. Crouse, C. Policar. *BioMetals*, **28**, 553 (2015).

[8] A. Gupte, R.J. Mumper. *Cancer Treat. Rev.*, **35**, 32 (2009).

[9] P.J. Jansson, P.C. Sharpe, P.V. Bernhardt, D.R. Richardson. *J. Med. Chem.*, **53**, 5759 (2010).

[10] P.S. Donnelly. *Dalton Trans.*, **40**, 999 (2011).

[11] U. Jungwirth, C.R. Kowol, B.K. Keppler, C.G. Hartinger, W. Berger, P. Heffeter. *Antioxid. Redox Signal.*, **15**, 1085 (2011).

[12] J. Wu, X. Hua. *Cancer Biol. Ther.*, **6**, 646 (2007).

[13] P.P. Silva, W. Guerra, J.N. Silveira, A.M.D.C. Ferreira, T. Bortolotto, F.L. Fischer, H. Terenzi, A. Neves, E.C. Pereira-Maia. *Inorg. Chem.*, **50**, 6414 (2011).

[14] P.R. Reddy, N. Raju. *Polyhedron*, **44**, 1 (2012).

[15] P.R. Chetana, R. Rao, S. Saha, R.S. Policegoudra, P. Vijayan, M.S. Aradhya. *Polyhedron*, **48**, 43 (2012).

[16] M. Chikira, C.H. Ng, M. Palaniandavar. *Int. J. Mol. Sci.*, **16**, 22754 (2015).

[17] D. İnci, R. Aydın, Ö. Vatan, D. Yılmaz, H.M. Gençkal, Y. Zorlu, T. Cavaş. *Spectrochim. Acta A: Mol. Biomol. Spectrosc.*, **145**, 313 (2015).

[18] X. Liu, X. Li, Z. Zhang, Y. Dong, P. Liu, C. Zhang. *Biol. Trace Elem. Res.*, **154**, 150 (2013).

[19] S.R. Liao, X.Y. Le, X.L. Feng. *J. Coord. Chem.*, **61**, 847 (2008).

[20] N. Aliaga-Alcalde, P. Marqués-Gallego, M. Kraaijkamp, C. Herranz-Lancho, H. den Dulk, H. Go□rner, O. Roubeau, S.J. Teat, T. Weyhermu□ller, J. Reedijk. *Inorg. Chem.*, **49**, 9655 (2010).

[21] R. Loganathan, S. Ramakrishnan, M. Ganeshpandian, N.S. Bhuvanesh, M. Palaniandavar, A. Riyasdeen, M.A. Akbarsha. *Dalton Trans*., **44**, 10210 (2015).

[22] T. Ma, J. Xu, Y. Wang, H. Yu, Y. Yang, Y. Liu, W. Ding, W. Zhu, R. Chen, Z. Ge, Y. Tan, L. Jia, T. Zhu. *J. Inorg. Biochem*., **144**, 38 (2015).

[23] S. Frankland-Searby, S.R. Bhaumik. *Biochim. Biophys. Acta (BBA)-Rev. Cancer*, **1825**, 64 (2012).

[24] S.S. Hindo, M. Frezza, D. Tomco, M.J. Heeg, L. Hryhorczuk, B.R. McGarvey, Q.P. Dou, C.N. Verani. *Eur. J. Med. Chem*., **44**, 4353 (2009).

[25] J. Adams. *Nat. Rev. Cancer*, **4**, 349 (2004).

[26] A. Paugam, A.L. Baulteau, J. Dupouy-Camet, C. Creuzet, B. Friguet. *Trends Parasitol*., **19**, 55 (2003).

[27] K. Ghosh, P. Kumar, V. Mohan, U.P. Singh, S. Kasiri, S.S. Mandal. *Inorg. Chem*., **51**, 3343 (2012).

[28] S. Tardito, O. Bussolati, M. Maffini, M. Tegoni, M. Giannetto, V. Dall'Asta, R. Franchi-Gazzola, M. Lanfranchi, M.A. Pellinghelli, C. Mucchino, G. Mori, L. Marchiò. *J. Med. Chem*., **50**, 1916 (2007).

[29] R. Loganathan, S. Ramakrishnan, E. Suresh, A. Riyasdeen, M.A. Akbarsha, M. Palaniandavar. *Inorg. Chem*., **51**, 5512 (2012).

[30] F.G. Hamel, J.L. Upward, G.L. Siford, C.W. Duckworth. *Metabolism*, **52**, 810 (2003).

[31] C. Detoni, N.M. Carvalho, D.A. Aranda, B. Louis, O.A.C. Antunes. *Appl. Catal. A. Gen*., **365**, 281 (2009).

[32] C.H. Ng, H.K.A. Ong, C.W. Kong, K.K. Su, S.W. Ng. *J. Coord. Chem*., **59**, 1089 (2006).

[33] H.L. Seng, K.W. Tan, M.J. Maah, W.T. Tan, H. Hamada, M. Chikira, C.H. Ng. *Polyhedron*, **28**, 2219 (2009).

[34] P. CRYSALIS. *Software system*, Agilent Technologies (2014).

[35] G.M. Sheldrick. *Acta Crystallogr., Sect. A*, **64**, 112 (2007).

[36] G.M. Sheldrick. *Acta Crystallogr., Sect. C*, **71**, 3 (2015).

[37] T.Y. Lin, C.H. Wu. *J. Catal*., **232**, 117 (2005).

[38] C.H. Ng, H.K.A. Ong, C.W. Kong, K.W. Tan, R.N.Z.R.A. Rahman, B.M. Yamin, S.W. Ng. *Polyhedron*, **25**, 3118 (2006).

[39] T. Mosmann. *J. Immunol. Methods*, **65**, 55 (1983).

[40] T. Sugimori, H. Masuda, N. Ohata, K. Koiwai, A. Odani, O. Yamauchi. *Inorg*. *Chem*., **36**, 576 (1997).

[41] H.L. Seng, W.S. Wang, S.M. Kong, H.K.A. Ong, Y.F. Win, R.N.Z.R.A. Rahman, M. Chikira, W.K. Leong, M. Ahmad, S.B.A. Khoo, C.H. Ng. *Biometals*, **25**, 1061 (2012).

[42] X. Li, Z. Zhang, C. Wang, T. Zhang, K. He, F. Deng. *J*. *Inorg*. *Biochem*., **105**, 23 (2011).

[43] C.H. Ng, W.S. Wang, K.V. Chong, Y.F. Win, K.E. Neo, H.B. Lee, S.L. San, R.N.Z.R.A. Rahman, W.K. Leong. *Dalton Trans*., **42**, 10233 (2013).

[44] M. Devereux, D. O'Shea, M. O'Connor, H. Grehan, G. Connor, M. McCann, G. Rosair, F. Lyng, A. Kellett, M. Walsh, D. Egan, B. Thati. *Polyhedron*, **26**, 4073 (2007).

[45] J.W. Lai, C.W. Chan, C.H. Ng, I.H. Ooi, K.W. Tan, M.J. Maah, S.W. Ng. *J*. *Mol*. *Struct*., **1106**, 234 (2016).

[46] C.W. Chan, J.W. Lai, I.H. Ooi, H.M. Er, S.M. Chye, K.W. Tan, S.W. Ng, M.J. Maah, C.H. Ng. *Inorg*. *Chim*. *Acta*, **450**, 202 (2016).

[47] S.E. Balaghi, E. Safaei, M. Rafiee, M.H. Kowsari. *Polyhedron*, **57**, 94 (2012).

[48] R. Calvo, R.P. Sartoris, H.L. Calvo, E.F. Chagas, R.E. Rapp. *Solid State Sci*., **55**, 144 (2016).

[49] S.I. Levchenkov, I.N. Shcherbakov, L.D. Popov, V.V. Lukov, V.V. Minin, Z.A. Starikova, E.V. Ivannikova, A.A. Tsaturvan, V.A. Kogan. *Inorg*. *Chim*. *Acta*, **405**, 169 (2013).

[50] G. Bhargavi, M.V. Rajasekharan, J.–P. Tuchagues. *Inorg*. *Chim*. *Acta*, **362**, 3247 (2009).

[51] K.R. O'Neal, T.V. Brinzari, J.B. Wright, C.L. Ma, S. Giri, J.A. Schlueter, Q. Wang, P. Jena, Z.X. Liu, J.L. Musfeldt. *Nat*. *Sci*. *Rep*., **4**, 1 (2014). http://dx.doi.org/10.1038/srep06054.

[52] A. Kufenicki, M. Świątek, M. Woźniczka, U. Kalinowska-Lis, J. Jezierska, J. Ochocki. *J. Solution Chem*., **45**, 28 (2016).

[53] A. Onder, M. Turkyilmaz, Y. Baran. *Inorg*. *Chim*. *Acta*, **391**, 28 (2012).

[54] S.T. Von, H.L. Seng, H.B. Lee, S.W. Ng, Y. Kitamura, M. Chikira, C.H. Ng. *J*. *Inorg*. *Biochem*., **17**, 57 (2012).

[55] S. Lutsenko, A. Gupta, J.L. Burkhead, V. Zuzel. *Arch*. *Biochem*. *Biophys*., **476**, 22 (2008).

[56] S.L. Fontaine, J.F.B. Mercer. *Arch*. *Biochem*. *Biophys*., **463**, 149 (2007).

[57] M. Reth. *Nat. Immunol.*, **3**, 1129 (2002).

[58] M.L. Low, L. Maigre, P. Dorlet, R. Guillot, J.M. Pages, K.A. Crouse, C. Policar, N. Delsuc. *Bioconjugate Chem.*, **25**, 2269 (2014).

[59] A. Kazi, S. Ozcan, A. Tecleab, Y. Sun, H.R. Lawrence, S.M. Sebti. *J. Biol. Chem.*, **289**, 11906 (2014).

[60] M.N. Aminake, H.D. Arndt, G. Pradel. *Int. J. Parasitol. Drugs Drug Resist.*, **2**, 1 (2012).

[61] G. Sava, A. Bergamo, P.J. Dyson. *Dalton Trans.*, **40**, 9069 (2011).

[62] A. Nencioni, F. Grünebach, F. Patrone, A. Ballestrero, P. Brossart. *Leukemia*, **21**, 30 (2007).

[63] G. Lin, D. Li, L.P.S. de Carvalho, H. Deng, H. Tao, G. Vogt, K. Wu, J. Schneider, T. Chidawanyika, J.D. Warren, H. Li, C. Nathan. *Nature*, **461**, 621 (2009).

[64] Z. Zhang, C. Bi, S.M. Schmitt, Y. Fan, L. Dong, J. Zuo, Q.P. Dou. *J. Biol. Inorg. Chem.*, **17**, 1257 (2012).

[65] A. Canepa, J.C. Divino Filho, A. Gutierrez, A. Carrea, A.M. Forsberg, E. Nilsson, E. Verrina, F. Perfumo, J. Bergström. *Nephrol. Dial. Transplant.*, **17**, 413 (2002).

[66] S. Zhai, L. Yang, Q.C. Cui, Y. Sun, Q.P. Dou, B. Yan. *J. Biol. Inorg. Chem.*, **15**, 259 (2010).

[67] M.N.M. Milunovic, E.A. Enyedy, N.R. Nagy, T. Kiss, R. Trondl, M.A. Jakupec, B.K. Keppler, R. Krachler, G. Novitchi, V.B. Arion. *Inorg. Chem.*, **51**, 9309 (2012).

[68] F. Bacher, E.A. Enyedy, N.R. Nagy, A. Rockenbauer, G.M. Bognar, R. Trondl, M.S. Novak, E. Klapproth, T. Kiss, V.B. Arion. *Inorg. Chem.*, **52**, 8895 (2013).

[69] N.J. Farrer, P.J. Sadler, *Bioinorganic Medicinal Chemistry*, E. Alessio (Ed.), Wiley-VCH, Weinheim (2011), pp. 1-47.

[70] A.C. Mirabella, A.A. Pletnev, S.L. Downey, B.I. Florea, T.B. Shabaneh, M. Britton, M. Verdoes, D.V. Filippov, H.S. Overkleeft, A.F. Kisselev. *Chem. Biol.*, **18**, 608 (2011).

[71] P.P. Geurink, W.A. van der Linden, A.C. Mirabella, N. Gallastegui, G. de Bruin, A.E. Blom, M.J. Voges, E.D. Mock, B.I. Florea, G.A. van der Marel, C. Driessen, M. van der Stelt, M. Groll, H.S. Overkleeft, A.F. Kisselev. *J. Med. Chem.*, **56**, 1262 (2013).

[72] A.F. Kisselev, W.A. van der Linden, H.S. Overkleeft. *Chem. Biol.*, **19**, 99 (2012).

[73] G. Yang, S. Nowsheen, K. Aziz, A.G. Georgakilas. *Pharmacol. Ther.*, **139**, 392 (2013).

[74] K. Barabas, R. Milner, D. Lurie, C. Adin. *Vet. Comp. Oncol.*, **6**, 1 (2008).

[75] R.H. Shoemaker. *Nat. Rev. Cancer*, **6**, 813 (2006).

[76] N. Alami, Z. Li, J. Engel, B. Leyland-Jones. *Cancer Res.*, **67**, 4780 (2007).

[77] A.E. Rashad, S.E. Gaballa, A.I. Hashem, D.A. Osman, M.M. Ali, S.F. Hamid, F.M.E. Abdel-Megeid. *Der Pharma Chem.*, **6**, 88 (2014).

[78] X. Zeng, L. Xiang, C.Y. Li, Y. Wang, G. Qiu, Z.X. Zhang, X. He. *Fitoterapia*, **83**, 609 (2012).

[79] J. Qi, S. Liang, Y. Gou, Z. Zhang, Z. Zhou, F. Yang, H. Liang. *Eur. J. Med. Chem.*, **96**, 360 (2015).

[80] S. Kathiresan, R. Dhivya, M. Vigneshwar, M. Rajasekaran, J. Ranjani, J. Rajendhran, S. Srinivasan, S. Mugesh, M. Murugan, P. Athappan, J. Annaraj. *J. Coord. Chem.*, **69**, 238 (2016).

[81] G.H. Sheng, Q.C. Zhou, X.M. Hu, C.F. Wang, X.F. Chen, D. Xue, K. Yan, S.S. Ding, J. Wang, Z.Y. Du, Z.H. Liu, C.Y. Zhang, H.L. Zhu. *J. Coord. Chem.*, **68**, 1571 (2015).

[82] X.T. Zhang, Z.Y. Ma, C. Zhao, C.Z. Xie, J.Y. Xu. *J. Coord. Chem.*, **68**, 2307 (2015).

[83] J.L. Li, L. Jiang, S.T. Li, J.L. Tian, W. Gu, X. Liu, S.P. Yan. *J. Coord. Chem.*, **67**, 3598 (2014).

[84] C. Slator, N. Barron, O. Howe, A. Kellett. *ACS Chem. Biol.*, **11**, 159 (2016).

[85] C.H. Ng, S.M. Kong, Y.L. Tiong, M.J. Maah, N. Sukram, M. Ahmad, A.S.B. Khoo. *Metallomics*, **6**, 892 (2014).

[86] D. Krajčiová, M. Melník, E. Havránek, A. Forgácsová, P. Mikuš. *J. Coord. Chem.*, **67**, 1493 (2014).

[87] S.S. Hindo, M. Frezza, D. Tomco, M.J. Heeg, L. Hryhorczuk, B.R. McGarvey, Q. Ping Dou, C.N. Verani. *Eur. J. Med. Chem.*, **44**, 4353 (2009).

[88] A. Kazi, K.G. Daniel, D.M. Smith, N.B. Kumar, Q. Ping Dou. *Biochem. Pharmacol.*, **66**, 965 (2003).

[89] K.G. Daniel, P. Gupta, R.H. Harbach, W.C. Guida, Q. Ping Dou. *Biochem. Pharmacol.*, **67**, 1139 (2004).

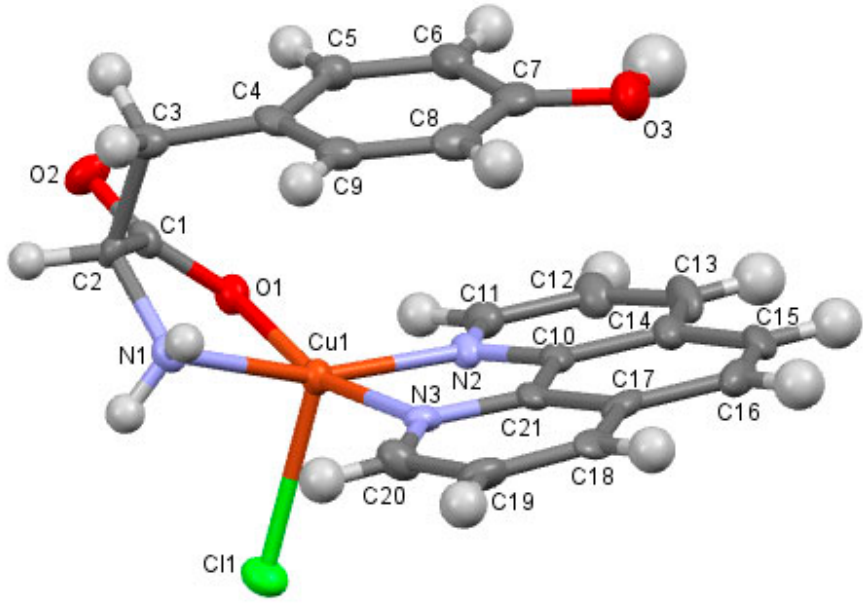

Figure 1a

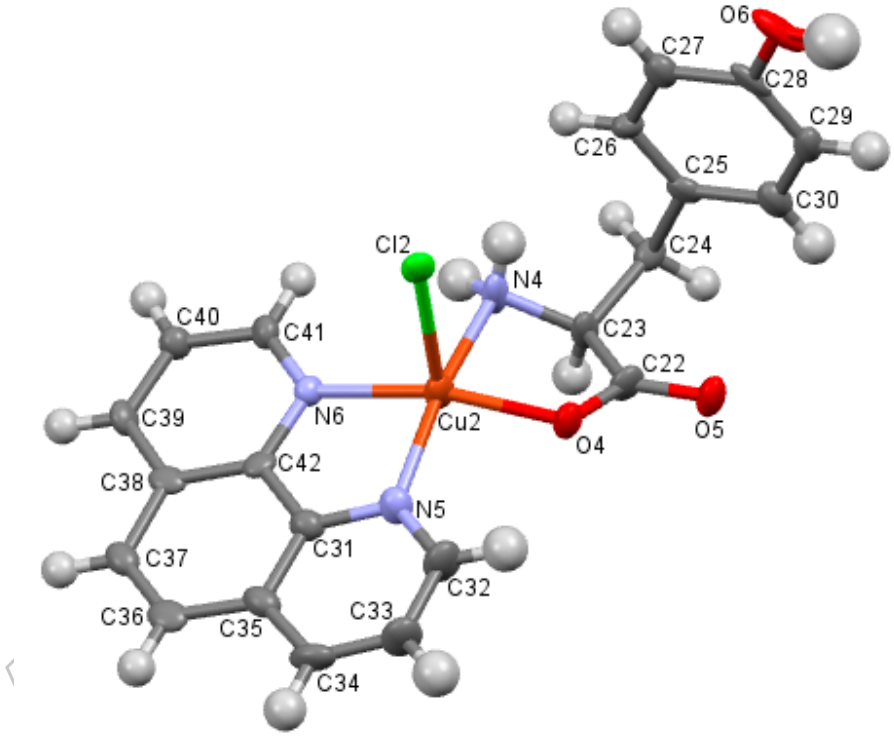

Figure 1b

Figure 1(a) and (b). ORTEP plots of two asymmetric molecules (a) and (b) of [Cu(phen)(L-tyr)Cl] (lattice water molecules are not shown for clarity).

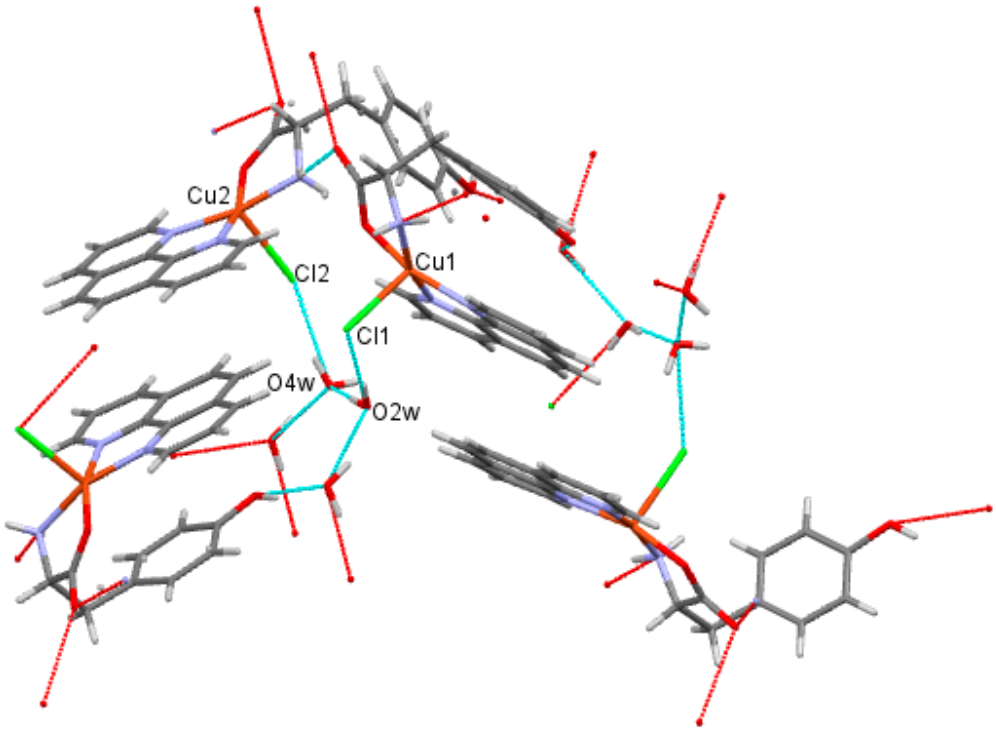

Figure 2. Hydrogen bonding network in the crystal lattice of [Cu(phen)(L-tyr)Cl]·2H_2O, showing the intermolecular H-bond linkage (blue lines) of the chloride (green; Cl1) of one molecule with the chloride (green; Cl2) of another adjacent molecule *via* the two lattice water molecules (Ow2 and Ow4).

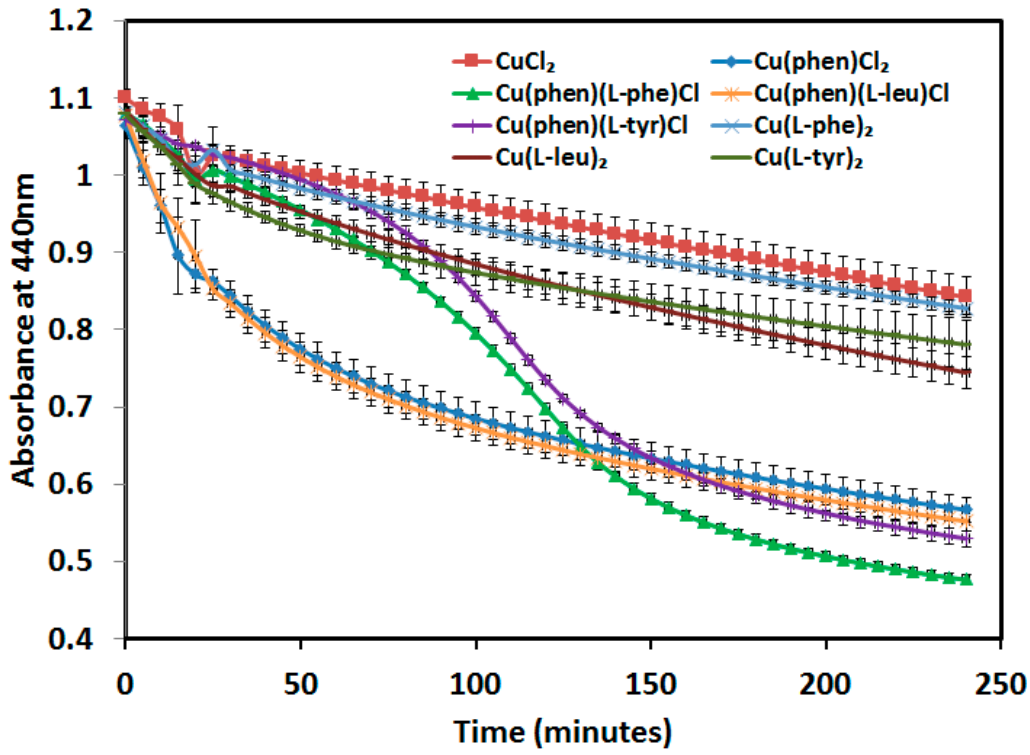

Figure 3a

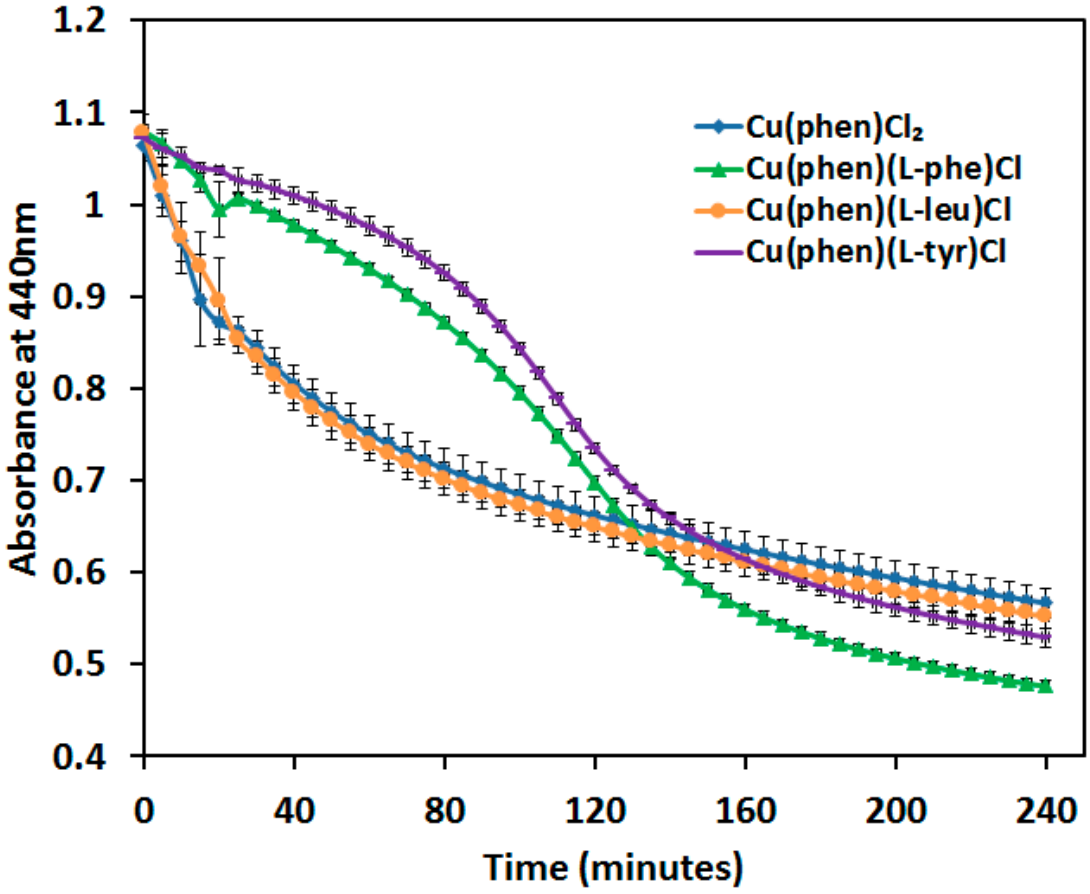

Figure 3b

Figure 3. Plot of absorbance of PNDA at 440 nm against time for (a) all the Cu(II) compounds (top) and (b) four Cu(II)-phen complexes (bottom).

Table 1. Crystal data and refinement parameters of [Cu(phen)(L-tyr)Cl]·2H_2O.

Empirical formula	$C_{21}H_{22}ClCuN_3O_5$
M_r	495.42
Crystal size, mm^3	0.40 × 0.40 × 0.10
Crystal system	Monoclinic
Space group	*P* 2_1
a, Å	11.6174(8)
b, Å	16.2035(12)
c, Å	11.7564(9)
α, °	90
β, °	102.061(7)
γ, °	90
Cell volume, $Å^3$	2164.2(3)
Z	4
T, K	100(2)
F_{000}	1060
μ, mm^{-1}	1.18
θ range, °	3.5 – 26.3
Reflections collected	12396
Reflections unique	6721
R_{int}	0.052
GOF	1.02
Refl. obs. (I>2σ(I))	5530
Parameters	567
wR_2 (all data)	0.124
R value (I>2σ(I))	0.050
Largest diff. peak and hole (e-.$Å^{-3}$)	1.38 and -0.52

Table 2. Selected bond distances (Å) and angles (°) for the two asymmetric units, (a) and (b), of [Cu(phen)(L-tyr)Cl]·2H_2O.

Molecule (a)		Molecule (a)		Molecule (b)	
Cu(1)-O(1)	1.981(4)	O(1)-Cu(1)-N(2)	91.5(2)	O(4)-Cu(2)-N(4)	82.3(2)
Cu(1)-N(2)	1.997(5)	O(1)-Cu(1)-N(1)	82.54(19)	O(4)-Cu(2)-N(5)	92.1(2)
Cu(1)-N(1)	2.011(5)	N(2)-Cu(1)-N(1)	163.0(2)	N(4)-Cu(2)-N(5)	169.6(3)
Cu(1)-N(3)	2.015(5)	O(1)-Cu(1)-N(3)	164.4(2)	O(4)-Cu(2)-N(6)	164.2(2)
Cu(1)-Cl(1)	2.5146(18)	N(2)-Cu(1)-N(3)	81.5(2)	N(4)-Cu(2)-N(6)	101.1(2)
Molecule (b)		N(1)-Cu(1)-N(3)	100.1(2)	N(5)-Cu(2)-N(6)	82.0(2)
Cu(2)-O(4)	1.952(5)	O(1)-Cu(1)-Cl(1)	97.05(14)	O(4)-Cu(2)-Cl(2)	98.4(14)
Cu(2)-N(4)	1.986(6)	N(2)-Cu(1)-Cl(1)	102.62(16)	N(4)-Cu(2)-Cl(2)	86.3(2)
Cu(2)-N(5)	2.003(6)	N(1)-Cu(1)-Cl(1)	93.89(17)	N(5)-Cu(2)-Cl(2)	103.3(2)
Cu(2)-N(6)	2.025(5)	N(3)-Cu(1)-Cl(1)	98.10(16)	N(6)-Cu(2)-Cl(2)	97.2(2)
Cu(2)-Cl(2)	2.543(4)				

Table 3. Molar conductivities of 1 mM Cu(II) complexes.

Compound	0 h	24 h	48 h
$[Cu(phen)Cl_2]$	123.6	130.9	130.2
$[Cu(phen)(L\text{-}phe)Cl]\cdot 3H_2O$	47.2	49.3	49.3
$[Cu(phen)(L\text{-}leu)Cl]\cdot 4½H_2O$	39.8	45.1	45.5
$[Cu(phen)(L\text{-}tyr)Cl]\cdot 3H_2O$	43.2	45.2	45.0
$[Cu(phe)_2]\cdot ½H_2O$	n.a.*	n.a.	n.a.
$[Cu(leu)_2]\cdot ½H_2O$	n.a.	n.a.	n.a.
$[Cu(tyr)_2]\cdot H_2O$	n.a.	n.a.	n.a.

*n.a. = cannot be determined due to poor solubility

Table 4. Production of •OH radicals, from reaction of compounds with H_2O_2, as measured by bleaching of PNDA*.

Compound	% of PNDA bleaching at different time (minutes)						
	20	40	80	120	160	200	240
$CuCl_2$	9.0	8.0	10.7	13.4	17.5	19.2	21.4
Phen	6.2	5.8	6.2	6.5	7.2	7.7	7.5
$Cu(phen)Cl_2$	18.3	24.3	32.5	36.7	41.3	42.9	44.7
$Cu(phen)(L\text{-}phe)Cl\cdot 3H_2O$	7.9	9.4	18.8	34.3	47.1	51.8	53.8
$Cu(phen)(L\text{-}leu)Cl\cdot 4½H_2O$	17.1	26.1	34.4	38.7	42.2	44.9	46.7
$Cu(phen)(L\text{-}tyr)Cl\cdot 3H_2O$	3.4	5.8	13.2	30.4	41.6	46.3	48.6
$Cu(L\text{-}phe)_2\cdot ½H_2O$	6.3	8.0	11.5	14.2	17.1	19.6	21.4
$Cu(L\text{-}leu)_2\cdot ½H_2O$	7.8	10.6	15.5	19.5	23.4	26.8	29.3
$Cu(L\text{-}tyr)_2\cdot H_2O$	8.5	12.3	16.7	19.4	22.0	24.1	25.5
L-phe	3.6	4.4	4.7	4.8	5.5	5.9	5.8
L-leu	4.7	4.1	4.6	5.2	6.2	7.0	7.2
L-tyr	3.9	4.7	4.9	5.1	5.7	6.1	6.0

* [•OH] is directly proportional to the % bleaching of the PNDA which is bleached quantitatively by •OH in a 1:1 ratio (PNDA: •OH)

Table 5. Concentration (μM) of the inhibitors that induced 50% inhibition of 20S proteasome activities.

Compound	IC_{50} (μM)		
	Trypsin-like	Chymotrypsin-like	Caspase-like
$CuCl_2$	1.5	7.0	2.0
Phen	>40	>40	>40
$[Cu(phen)Cl_2]$	3.5	33.3	12.7
$[Cu(phen)(L\text{-}phe)Cl]\cdot 3H_2O$	3.5	39.2	20
$[Cu(phen)(L\text{-}leu)Cl]\cdot 4½H_2O$	1.7	28.5	14.2
$[Cu(phen)(L\text{-}tyr)Cl]\cdot 3H_2O$	2.5	>40	10
$Cu(L\text{-}phe)_2\cdot ½H_2O$	1.7	>40	14.2
$Cu(L\text{-}leu)_2\cdot ½H_2O$	1.7	22	12.7
$Cu(L\text{-}tyr)_2\cdot H_2O$	1.7	17.5	7.2
L-phe	>40	>40	>40
L-leu	>40	>40	>40
L-tyr	>40	>40	>40
Epoxomicin	0.0025	0.0011	0.0047

Table 6. MTT assay (μM) for Cu(II) complexes on different cancer cell lines.

Compound	MCF7			HepG2			CNE1			A549		
	GI_{50}	TGI	LD_{50}	GI_{50}	TGI	LD_{50}	GI_{50}	TGI	LD_{50}	GI_{50}	TGI	LD_{50}
[Cu(phen)Cl_2]	1.4 ±0.3	3.7 ±0.2	4.8 ±0.3	1.3 ±0.4	3.8 ±0.4	6.6 ±0.7	1.1 ±0.4	1.9 ±0.4	5±1	1.0 ±0.5	2.0 ±0.3	6.3 ±0.3
[Cu(phen)(L-phe)Cl]·3H_2O	0.70 ±0.02	1.4 ±0.2	2.3 ±0.5	2.0 ±0.9	4.0 ±0.9	3.7 ±0.4	2.7 ±0.6	4.00 ±0.8	>10.00	0.9 ±0.4	2.0 ±0.5	3.4 ±0.9
[Cu(phen)(L-leu)Cl]·4½H_2O	1.1 ±0.5	2.9 ±0.4	3.5 ±0.4	1.1 ±0.5	2.1 ±0.8	>10.00	1.26 ±0.07	2.3 ±0.4	5.4 ±0.6	1.2 ±0.1	2.5 ±0.7	>10.00
[Cu(phen)(L-tyr)Cl]·3H_2O	0.70 ±0.06	1.5 ±0.2	4.7 ±0.4	3.7 ±0.2	8.0 ±0.7	>10.00	0.8 ±0.2	1.7 ±0.3	6.5 ±0.2	1.07 ±0.08	4.0 ±0.4	>10.00
Cu(L-phe)$_2$·½H_2O	>10.00	>10.00	>10.00	3.1 ±0.4	>10.00	>10.00	2.4 ±0.5	>10.00	>10.00	1.5 ±0.4	>10.00	>10.00
Cu(L-leu)$_2$·½H_2O	>10.00	>10.00	>10.00	>10.00	>10.00	>10.00	3.7 ±0.8	>10.00	>10.00	2.0 ±0.7	>10.00	>10.00
Cu(L-tyr)$_2$·H_2O	>10.00	>10.00	>10.00	>10.00	>10.00	>10.00	1.9 ±0.9	>10.00	>10.00	1.8 ±0.4	>10.00	>10.00

Graphical abstract